Relevant energy scale in hybrid mesoscopic Josephson junctions

Franco Carillo,[1,*] Detlef Born,[1,2] Vittorio Pellegrini,[1] Francesco Tafuri,[1,2] Giorgio Biasiol,[3] Lucia Sorba,[1] and Fabio Beltram[1]
[1]*NEST, INFM-CNR and Scuola Normale Superiore, I-56126 Pisa, Italy*
[2]*Coherentia, INFM-CNR and Dipartimento Ingegneria dell'Informazione, Seconda Universitá di Napoli, 81031 Aversa (CE), Italy*
[3]*NEST and Laboratorio Nazionale TASC, INFM-CNR, Area Science Park, I-34012 Trieste, Italy*
(Received 17 March 2008; revised manuscript received 26 May 2008; published 25 August 2008)

Transport properties of high quality Nb/semiconductor/Nb long Josephson junctions based on metamorphic $In_{0.75}Ga_{0.25}As$ epitaxial layers are reported. Different junction geometries and fabrication procedures are presented that allow a systematic comparison with quasiclassical theory predictions. The impact of junction transparency is highlighted and a procedure capable of yielding a high junction quality factor is identified.

DOI: 10.1103/PhysRevB.78.052506 PACS number(s): 73.23.−b, 74.45.+c

Superconductor/semiconductor hybrid devices are of much interest not only for their potential for electronic-device implementation but also as model systems for the investigation of the phenomena regulating the conversion of supercurrent into normal current at the interface through Andreev reflection.[1] By taking advantage of the increasing availability of ultrapure nanoscale semiconductors, major advances in the understanding of the microscopic nature of Josephson coupling and the interplay between superconductivity and mesoscopic effects are expected.[2–4] Recent examples are the demonstration of the control of Josephson current in diffusive InAs nanowires coupled to superconducting leads (J dot)[3] and the study of the interplay between quantum interference effects and superconducting correlation.[5,6] Arguably, the main limiting factor for the exploitation of hybrid systems in practical devices is the low value of the junction quality factor I_CR_N (i.e., critical current value times normal resistance). In fact, with a few exceptions,[7,8] this is the parameter normally referred to in the literature.[9–11] It is crucial to have the largest possible values of I_CR_N, since, for instance, the maximum voltage amplification that can be obtained from a Josephson field-effect transistor (FET) (Ref. 18) or a J dot is proportional to I_CR_N. The values of I_CR_N found in experimental works, however, are far from those predicted by theory. This raises several issues about the actual nature of these junctions and motivated transport analysis such as the one reported here.

The reduction of I_CR_N for semi/super Josephson junctions was already discussed in terms of reduced dimensionality of the normal conductor,[16] low transparency of semi/super interfaces,[17] diffusive interface,[10] and decoherence effects.[9]

In a recent work Hammer *et al.*[12] studied superconductor-normal-superconductor (SNS) junctions with nonideal S/N interfaces. These authors predicted that the Thouless energy (E_{Th}) is replaced by the proximity induced gap in the normal region as the relevant energy scale for proximity effect determining, for instance, the temperature dependence of the critical current. (In a diffusive system with ideal transparent interfaces $E_{Th}=\hbar D/L^2$).

The objective of our work is twofold: (i) to investigate experimentally the theoretical predictions on the impact of the actual transparency of SN interfaces on SNS systems, and (ii) to identify a processing strategy capable of yielding high quality junctions. We shall examine various junctions characterized by different transparencies and N regions of various length and compare experimental I_C vs T curves for different fabrication processes. From these curves, thanks to the knowledge of the parameters of N material, we shall be able to analyze our data in the frame of Ref. 12 and identify the process yielding the maximum interface transparency. In particular, we report a semiconductor/superconductor interface configuration for which I_CR_N is close to 0.5 mV for a junction length of 400 nm, among the best results ever obtained for such hybrid devices.

In the hybrid devices of interest here, the normal conductor is an epitaxial layer of $In_{0.75}Ga_{0.25}As$ bulk doped with silicon. Thickness is in the range of 50–200 nm. Structures were grown by molecular-beam epitaxy (MBE) on a GaAs (100)-oriented substrate.[13] A sequence of $In_xAl_{1-x}As$ layers of increasing In content was first deposited in order to ensure lattice matching with the upstanding layer of $In_{0.75}Ga_{0.25}As$. Before the Nb deposition, we performed a two-step surface cleaning of the semiconductor consisting of a first wet removal of the native oxide using diluted (1/50) HF solution and a subsequent vacuum rf discharge cleaning at very low power in argon. Nb was then sputtered *in situ* during the same vacuum cycle and electrodes were defined by lift-off. All Nb films were 85 nm thick. We shall call the device obtained with this process type "A:" It is schematically shown in Fig. 1(a). Type A (junctions J1 and J2 reported in Table I) was fabricated on a 200-nm-thick epilayer with charge density of 1.32×10^{24} m^{-3} and mobility of 0.69 $m^2/V\,s$ at 1.5 K in the dark. A second type of device was fabricated on 50-nm-thick epitaxial layers with charge density $n=2.52\times10^{24}$ m^{-3} and mobility $\mu=0.52$ $m^2/V\,s$. We defined the semiconductor geometry (junction width) by employing a negative e-beam resist as a mask and subsequent wet chemical etching in $H_2SO_4/H_2O_2/H_2O$ solution. This type of device is labeled "B" and is displayed in Fig. 1(b). A third type ["C," shown in Fig. 1(c)] of junction was obtained by realizing the semiconductor mesa before Nb deposition. A Ti mask is first defined on the substrate by e-beam lithography, Ti thermal evaporation, and lift-off. $In_{0.75}Ga_{0.25}As$ structures are then defined by reactive ion etching. The last step is Nb deposition using the same technique described for type A. For type C we employed the same epitaxial layers of type B. For all samples the transition temperature of Nb leads is $T_c=8.7$ K, from which, using the formula $\Delta_S=\Delta_{Nb}=1.9\ k_BT_c$, we calculate the gap of the superconductor $\Delta_{Nb}=1.37$ mV.

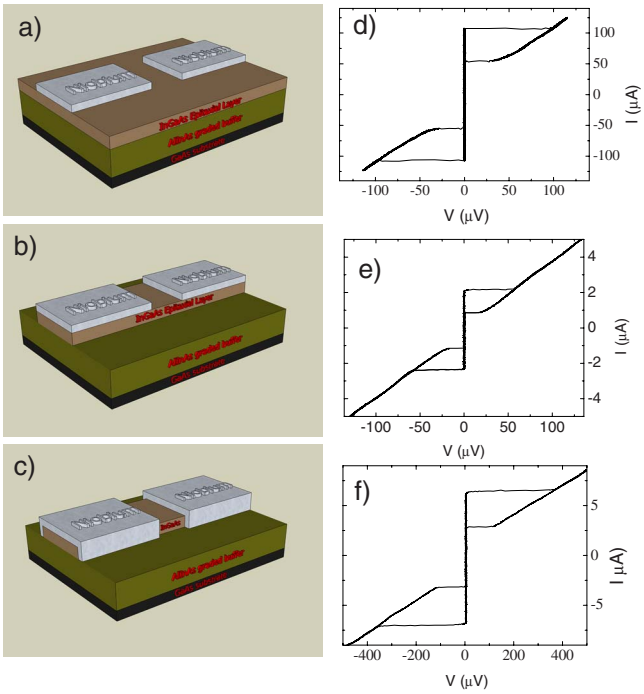

FIG. 1. (Color online) Panels (a), (b), and (c) report schemes of type-A, -B, and -C junctions, respectively, from the bottom layer: GaAs substrate (black), $In_xAl_{1-x}As$ graded buffer, $In_{0.75}Ga_{0.25}As$ epitaxial layer, and niobium (gray). Panels (d), (e), and (f) show *I-V* curves at $T=250$ mK of junctions J1, J4, and J5 (see Table I).

Measurements were performed as a function of temperature down to 250 mK in an ^{3}He cryostat. Current and voltage leads were filtered by *RC* filters at room temperature. A second filtering stage consisted of *RC*+copper powder filters thermally anchored at 1.5–1.9 K. The last copper-powder filter stage was at 250 mK, thermally anchored to the ^{3}He pot. The shielding from magnetic field was ensured by a combination of nested cryoperm, Pb, and Nb foils with all of them placed in the measurement Dewar and immersed in liquid ^{4}He.

In all junctions, with normal conductor lengths L typically ranging between 250 nm and 1.1 μm, we found a measurable supercurrent; see Fig. 1 panels (d)–(f). For type-A structures, we measured the critical current in different junctions made on the same chip (the same transparency was assumed in this case). These junctions had different values of electrode gap (1.1 μm–250 nm) and, as a consequence, of barrier length. Data are consistent with an exponential decrease in I_C vs L such as in metallic SNS.[14] The Fraunhofer-type patterns shown in Fig. 2 confirm the Josephson nature of the zero voltage current. The period measured for junctions of different widths and lengths is consistent with theoretical expectations, which take into account flux focusing effects.[15] The critical current was evaluated using a 1 μV criterion, while R_N was determined from a linear fit of *I-V* curves at $V>3$ mV.

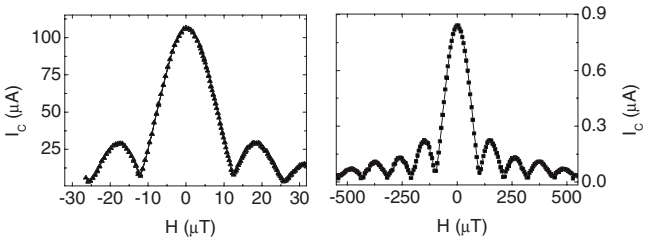

FIG. 2. Critical current (I_C) vs magnetic field (H) $T=250$ mK for a type-A junction with $W=20$ μm and $L=250$ nm (left) and a type-B junction with $W=5$ μm and $L=900$ nm (right).

For short ($\frac{\Delta_S}{E_{\rm Th}} \to 0$) and tunnel junctions, the only relevant energy scale is Δ_S and at low temperature I_CR_N saturates at the value of $\frac{1.326\pi\Delta_S}{2e}$. In the ideal case of SN interfaces with zero resistance and very long junctions ($\frac{\Delta_S}{E_{\rm Th}} > 100$), $E_{\rm Th}$ determines both the value at which I_CR_N saturates at $T \to 0$ and the characteristic temperature of its exponential decrease. In this limit I_CR_N is not related to Δ_S but only to $E_{\rm Th}$ through the expression $I_CR_N = bE_{\rm Th}$, where $b=10.52$. While the ratio $\frac{\Delta_S}{E_{\rm Th}}$ decreases, b gets smaller. The complete curve of I_CR_N as a function of $\frac{\Delta_S}{E_{\rm Th}}$ is reported in Ref. 14. The proportionality between I_CR_N and $E_{\rm Th}$ for very long junctions was experimentally demonstrated in the case of metallic SNS with transparent SN barriers.[14] For increasing SN interface resistance, Hammer *et al.*[12] showed that I_C vs T curves change their concavity from downward to upward and the energy scale of their temperature decay is determined by an effective Thouless energy ($E^*_{\rm Th}$) which depends on the ratio r between the resistance of the SN interfaces and the resistance of the normal conductor. In Ref. 12 is shown that for $\Delta_S/E_{\rm Th} \to \infty$ and large r ($r>10$) the following approximate relation holds: $E^*_{\rm Th}/E_{\rm Th} = {\rm Ar}^B/(C+r)$, where A, B, and C are parameters which fit the numerical solutions and depend on

TABLE I. $(I_CR_N)_{\rm theor}$ is a theoretical estimate made on the basis of $E^\star_{\rm Th}$. Both $(I_CR_N)_{\rm theor}$ and (I_CR_N) are taken at 250 mK (see text).

	Type	W (μm)	L (nm)	J_C (A/cm^2)	$E_{\rm Th}$ (μeV)	$E^*_{\rm Th}$ (μeV)	$(I_CR_N)_{\rm theor}$ (mV)	I_CR_N (mV)	$(I_CR_N)_{\rm theor}/I_CR_N$ ($T=250$ mK)
J1	A	20	250	2.68×10^3	545	23	0.205	0.101	2.0
J2	A	20	800	4.35×10^2	53	10	0.074	0.030	2.5
J3	B	10	800	1.18×10^3	52	14	0.124	0.079	1.6
J4	B	5	900	8.96×10^2	49	16	0.149	0.059	2.5
J5	C	0.45	400	2.84×10^4	284	284[a]	1.16	0.470	2.5
J6	C	0.40	800	5.05×10^4	62	62[a]	0.493	0.303	1.6

[a]$E^*_{\rm Th}$ has been taken equal to $E_{\rm Th}$; see text.

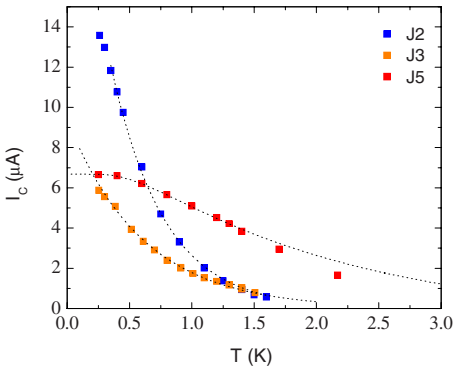

FIG. 3. (Color online) I_C vs T data points for junctions J2, J3, and J5 (symbols) along with the theoretical fit (dotted lines).

Δ_S/E_{Th}. We introduce E^*_{Th} in our discussion to have a single modeling parameter that has as its only purpose to account for barrier properties. As the effective Thouless energy becomes smaller, the value of $I_C R_N$ at low temperatures also becomes smaller and the decrease of I_C at high temperatures faster. A reduced effective value of E_{Th} also implies a larger value of the ratio . In other words, the junction gets longer as r increases. In our paper, in agreement with Ref. 12, we link the temperature decay of I_C to E^*_{Th} and show that the latter value also determines the size of $I_C R_N$ at low temperature.

In order to provide an estimate of E^*_{Th}, we measured I_C vs T curves for all junctions. Three representative results (filled points) are shown in Fig. 3. $I_C(T)$ can be well approximated by an exponential function for sufficiently long junctions and high temperatures ($k_B T > 5E_{\mathrm{Th}}$):

$$I_C(T) \propto \exp(-T/T^*), \tag{1}$$

where T^* is linked to the Thouless energy of the system by $E^*_{\mathrm{Th}} = \frac{2\pi k_B T^*}{24}$.[14] We have used Eq. (1) to fit our data for all junctions of types A and B as shown in Fig. 3. The resulting values of $E^\star_{\mathrm{Th}}$ are reported in Table I. For these devices $E^\star_{\mathrm{Th}}$ is smaller than E_{Th}, which can be calculated from the relevant diffusion coefficients and junction lengths.

The values of the ratio $\Delta_{\mathrm{Nb}}/E^\star_{\mathrm{Th}}$ span from 60 to 170 and $k_B T \gg E^\star_{\mathrm{Th}}$ for all junctions in the temperature range considered in the fit ($T \geq 500$ mK), fully justifying the use of Eq. (1).[14] Our analysis of I_c vs T shows that type-A and -B junctions exhibit a behavior characteristic of much longer junctions with respect to their actual geometric length. I_C vs T corresponding to junctions of type C is remarkably different from those of other devices as shown in Fig. 3. The curve is concave downward and saturates at 250 mK. This curve shape is typical of junctions having SN interfaces with low barrier resistance (see Figure 6 in Ref. 12). For these devices, $T < E_{\mathrm{Th}}/k_B$ in the whole temperature range considered (low-temperature regime),[12,14] $I_C(T)$ can be approximated by $I_C = (aE_{\mathrm{Th}}/eR_N)(1 - ce^{-aE_{\mathrm{Th}}/3.2k_B T})$ (Ref. 14; R_N is 73.5 Ω for J5). An excellent fit is achieved with an effective Thouless energy of $E^*_{\mathrm{Th}} = 284$ μeV and the parameters $a = 1.979$ and $c = 1.45$. The quality of the fit, slightly deviating from the experimental data only for $T > 1.5$ K, confirms that the value of E^*_{Th} is comparable to E_{Th} as opposed to cases A and B. We speculate that the nature and/or the geometry of super-/semi-interface characterizing type C can yield higher effective Thouless energies. The reasons for which type-C interfaces have better performance are not quite clear but are probably originated by a different structure following the peculiar fabrication procedure. This last includes Ti mask deposition, reactive ion etching, and mask removal by HF solution. In this configuration an etched wire of small width (450 nm) is in contact with the superconductor not only on the top of the smooth mesa surface, such as in cases A and B, but also through the two sides, at the rough surface of the etched side walls. It is, however, not possible to ascribe with certainty the improvement of the interface to the top contact, to the side contact, or both. It is widely accepted that the relatively poor quality of S/N barriers is largely determined by reactive ion etching. Yet this is funded on data for junctions whose SN side contacts were taken on buried two-dimensional electron gases.[2,9] In those devices, contacts were made to the side of active layers less than 10 nm thick, which were charge populated by modulation doping. our junctions are based on bulk doped surface layer and are therefore quite different from most systems studied in the literature. Bulk doped structures such as ours are more robust, as compared to modulation doped quantum wells, to the formation of a charge depleted (dead) layer at the two sides of the mesa after dry etching. We believe that the rough surface of the side walls (which is still perfectly conducting in our case) promotes the adhesion of metallic films, thus improving effective contact area, and transparency. An inhomogeneous contact can present areas with different transparency: indeed the overall behavior of the junction is determined by those areas having a large transparency. Another mechanism worth of future investigation could be a possible change in the chemistry of the top surface in the epilayer due to deposition and subsequent removal of the Ti mask. A chemical reaction at the surface between the mask and the semiconductor could be favored, for instance, by local heating of the mask during the reactive ion etching (RIE).

In Table I we calculate theoretical expected $I_C R_N$ for J1–J6 after Ref. 14 on the basis of $E^\star_{\mathrm{Th}}$. We find for all junctions, including J5 and J6, a factor of 2 between theoretical and measured $I_C R_N$.[19] This confirms the effectiveness of the model described in Ref. 12. Our data systematically show that SNS systems with non-ideal SN interfaces can be characterized by an energy scale (E^*_{Th}) capable of accounting for barrier resistance and transport parameters simultaneously. Th other interesting result is the identification of a fabrication process for which E^*_{Th} is almost equal to E_{Th} (J5 and J6). The agreement of $I_C R_N$ with existing theory is not perfect for both high transparency junctions (J5) and low transparency junctions (J1–J4). A discrepancy with theory of the same order was also found in some works based on metallic SNS junctions[20,21] and attributed to spurious factors such as the effective area of the contact.[14]

Finally we note that J5 and J6 exhibit an $I_C R_N$ value very close to the maximum obtainable for the given geometry and material parameters for ideally transparent interfaces. To the best of our knowledge, similar results for semiconductor/superconductor devices were obtained only for junctions employing Si/Ge (Ref. 22) and InAs nanowires.[5] We remark that, differently from the last two cited works, our devices

are based on a standard top-down fabrication approach fully compliant with large scale integration. We stress that J5 and J6 have been fabricated on different samples in different times. For J6 HF cleaning was more concentrated (1/20 instead of 1/50) and the normal conductor was ring shaped. To calculate the supercurrent density for J6, we considered W as the sum of the widths of the two arms forming the ring. For the estimation of the Thouless energy, we considered L equal to one-half the average circumference of the ring plus the gap between Nb electrodes and the ring. High values of the characteristic voltage have been obtained on similar structures produced with the same fabrication process. These are mostly SNS junctions with ring-shaped normal conductor. Further details on SNS ring devices will be reported elsewhere.

In conclusion we showed that the quality of semi-/super interface does play a crucial role in determining the value of the effective Thouless energy in SNS junctions. The comparison of different junction architectures shows that the reduction in $I_C R_N$ is accompanied/mediated by the reduction in effective Thouless energy. We determined a junction configuration maximizing $I_C R_N$ and supercurrent density. This opens the way to the realization of charge-controlled devices (J dot) with critical currents larger than 10 nA.

We acknowledge useful discussions with A. Golubov, A. Tagliacozzo, and P. Lucignano. Financial support from EC within the FP6 project HYSWITCH (Grant No. FP6-517567) is acknowledged.

*franco.carillo@sns.it

[1] G. E. Blonder, M. Tinkham, and T. M. Klapwijk, Phys. Rev. B **25**, 4515 (1982).
[2] H. Takayanagi, T. Akazaki, and J. Nitta, Phys. Rev. Lett. **75**, 3533 (1995).
[3] J. van Dam, Y. Nazarov, E. Bakkers, S. De Franceschi, and L. Kouwenhoven, Nature (London) **442**, 667 (2006).
[4] K. Grove-Rasmussen, H. Ingerslev Jrgensen, and P. E. Lindelof, New J. Phys. **9**, 124 (2007).
[5] Y.-J. Doh, J. A. van Dam, A. L. Roest, E. P. A. M. Bakkers, L. P. Kouwenhoven, and S. De Franceschi, Science **309**, 272 (2005).
[6] F. Giazotto, P. Pingue, F. Beltram, M. Lazzarino, D. Orani, S. Rubini, and A. Franciosi, Phys. Rev. Lett. **87**, 216808 (2001).
[7] The few works that make exception to this are mainly based on very short junctions.
[8] A. Chrestin and U. Merkt, Appl. Phys. Lett. **70**, 23 (1997).
[9] Th. Schäpers, J. Malindretos, K. Neurohr, S. Lachenmann, A. van der Hart, G. Crecelius, H. Hardtdegen, H. Lüth, and A. A. Golubov, Appl. Phys. Lett. **73**, 2348 (1998).
[10] J. P. Heida, B. J. van Wees, T. M. Klapwijk, and G. Borghs, Phys. Rev. B **57**, R5618 (1998).
[11] K. W. Lehnert, N. Argaman, H.-R. Blank, K. C. Wong, S. J. Allen, E. L. Hu, and H. Kroemer, Phys. Rev. Lett. **82**, 1265 (1999).
[12] J. C. Hammer, J. C. Cuevas, F. S. Bergeret, and W. Belzig, Phys. Rev. B **76**, 064514 (2007).
[13] F. Capotondi, G. Biasiol, D. Ercolani, V. Grillo, E. Carlino, F. Romanato, and L. Sorba, Thin Solid Films **484**, 400 (2005).
[14] P. Dubos, H. Courtois, B. Pannetier, F. K. Wilhelm, A. D. Zaikin, and G. Schön, Phys. Rev. B **63**, 064502 (2001).
[15] J. Gu, W. Cha, K. Gamo, and S. Namba, J. Appl. Phys. **50**, 6437 (1979).
[16] V. Z. Kresin, Phys. Rev. B **34**, 7587 (1986).
[17] M. Yu. Kuprianov and V. F. Lukichev, Sov. Phys. JETP **67**, 1163 (1988).
[18] T. D. Clark, J. Appl. Phys. **51**, 2736 (1980).
[19] In geometry A normal current can flow outside the close interelectrode area, where supercurrent is confined, leading to a reduced value of R_N. Due to the favorable value of the ratio W/L, the underestimate of R_N is a small percent.
[20] L. Angers, F. Chiodi, G. Montambaux, M. Ferrier, S. Gueron, H. Bouchiat, and J. C. Cuevas, Phys. Rev. B **77**, 165408 (2008).
[21] H. Courtois, Ph. Gandit, and B. Pannetier, Phys. Rev. B **52**, 1162 (1995).
[22] Jie Xiang, A. Vidan, M. Tinkham, R. M. Westervelt, and Charles M. Lieber, Nat. Nanotechnol. **1**, 208 (2006).